Tailoring of gradient coils for numerical exposure evaluations based on experimentally measured B-field

F. Liu[1], A. Trakic[1], H. Sanchez Lopez[1], E. Weber[1], and S. Crozier[1]

[1]The School of Information Technology and Electrical Engineering, The University of Queensland, Brisbane, Queensland, Australia

Synopsis: Assessment of MRI worker exposures to pulsed magnetic fields produced by gradient coils has recently attracted a lot of awareness in the field of occupational health and safety. To accurately model the exposures, a full three-dimensional distribution of the magnetic field in the vicinity of the magnet end is required. Unfortunately, for many MRI installations, the coil pattern that generates this magnetic field is often not provided by the manufacturer. A method is presented in which the prediction of a current distribution that generates a nearly identical magnetic field pattern is constrained by a number of experimentally measured magnetic field sample points outside the gradient set of interest. The method takes into consideration other important descriptors such as field uniformity in the working volume, gradient coil geometry, driving current, gradient strength, active shielding etc. To demonstrate the application of the method, current density and matching magnetic field distributions of x- and z-axis gradient coils are derived. This enables robust, accurate evaluations of exposures of tissue-equivalent numerical worker models without pre-knowledge of gradient coil patterns.

Method: First, the magnetic field produced by the gradient coil of interest is measured at a number of locations near the magnet end using the ambulatory magnetic field dosimeter [1].

If the gradient set radii and lengths are not provided by the manufacturer, as it was the case of this study, the inner magnet bore diameter and overall length can be measured. Based on these measurements, the radial and axial dimensions of the primary and shielding gradient coil layers can be estimated. It is then sufficient to use the guesstimates as initial conditions in the optimization routine. The continuous current distributions on the primary and shielding layers were defined in terms of stream functions with a total of twelve coefficients (six for primary and six for shielding layer respectively). The radial and axial dimensions of the primary and shielding coil, and the stream function coefficients were optimized using the least-square (LS) optimization method. If however, all the gradient coil dimensions are known a priori, there is naturally no need to perturb these. A number of important constraints were enforced in the optimization process in order to assure practical solutions. For example, the primary and shielding coil radial and axial dimensions were appropriately bounded in respect to abovementioned inner magnet bore diameter and overall length, the diameter spherical volume (DSV) region was defined as R = 0.225 x Z = 0.225 m, the transport current and the target gradient field strength were assumed to be 400A and 30 mT/m respectively. To maximize the shielding effectiveness, the components of the magnetic field at r = 0.5m (main magnet as eddy current source) were minimized during the optimization procedure. To match the measured magnetic field pattern near the coil end, sufficient samples of the magnetic field were chosen within the designated X-Z-plane (Y=0) (see Fig.1).

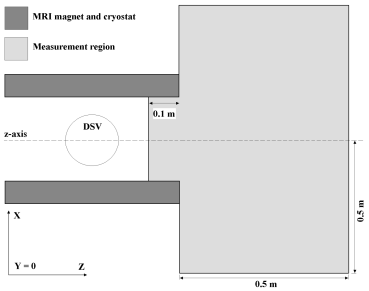

Fig.1-The illustration of measurement region for the switched gradients – X-Z plane.

Results and discussion: Figs.2 and 3 illustrate the wire patterns in the primary and shielding layers of the x and z-axis gradient coils respectively.

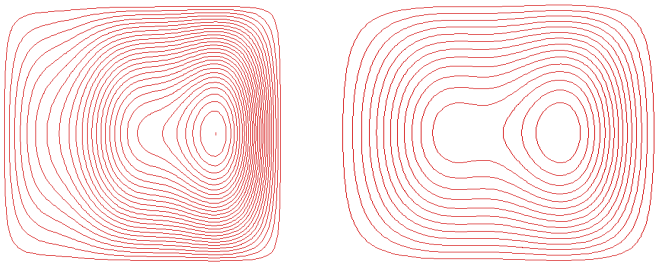

Fig.2 – X-axis gradient coil wire pattern: ½ primary (left) and ½ shielding coil (right).

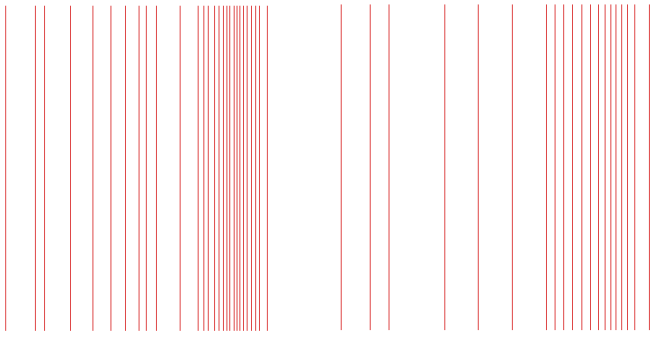

Fig.3 – Z-axis gradient coil wire pattern: ½ primary (left) and ½ shielding coil (right).

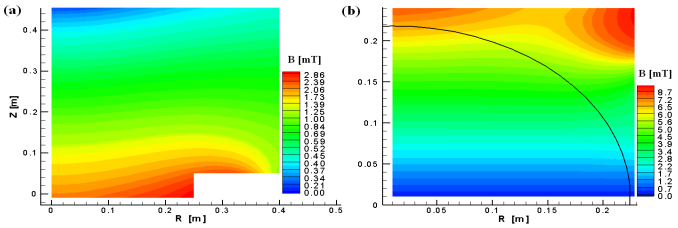

Fig.4 – **(a)** X-gradient B-field near coil end, **(b)** z-gradient coil DSV uniformity.

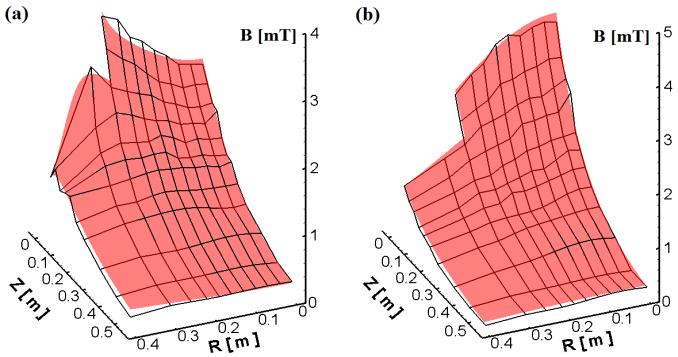

Fig.5 – Comparison of the measured (mesh) and optimised (red) magnetic field profiles near the coil end: **(a)** x-axis and **(b)** z-axis gradient coil. The field distributions are in good agreement.

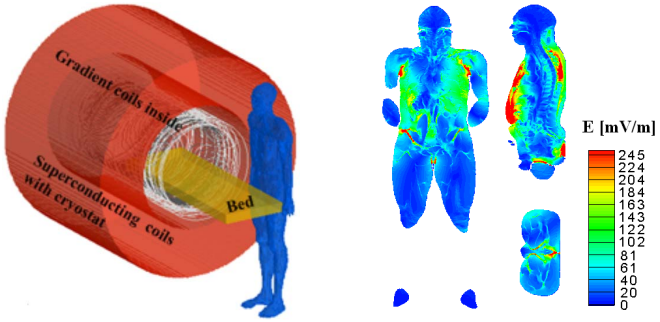

Fig.6 – Application example: **(a)** Location of the 2mm-resolution tissue-equivalent numerical worker model [2] near the combination of switched x-axis and z-axis gradient coils (1kHz trapezoidal switching, 250μs gradient rise time, 30mT/m gradient field strength in the working volume). The surface of the model is 1cm away from the gradient coil set and patient bed respectively. The patient bed is assumed to be 0.4m in width. The tissue conductivities were appropriately scaled to the frequencies of gradient operation; **(b)** Shown are distribution and levels of electric fields induced in the model worker in axial, coronal and sagittal planes. The details of the numerical solver are given in [3].

Based on a number of experimentally measured B-field sample points near the coil end, it is possible to optimise the current density distributions on the primary and shielding layer in order to match the measured B-field distribution whilst taking into account other practical gradient coil constraints. Using the derived current density distributions it is then feasible to compute the vector magnetic potential or B-field pattern (depending on the numerical solver) inside an tissue-equivalent body model of MRI worker near the coil end and thus to numerically evaluate the levels/profiles of induced E- fields.

Conclusion: A method was presented that enables more accurate computations and predictions of worker exposures in MRI settings without detailed electromagnetic source - gradient coil patterns.

Acknowledgements: Financial support from the Australian Research Council is gratefully acknowledged.

References:

[1] A Magnetic Field Dosimeter - PCT/AU2005/001495.
[2] Brooks Air-force Model - www.brooks.af.mil/AFRL/HED/hedr/dosimetry.html.
[3] F. Liu *et. al.*, IEEE Transactions on Biomedical Engineering, 50 (7): 804-815, 2003.
[4] R. Turner, Magnetic Resonance Imaging, vol. 11, pp. 903-20, 1993.